AJNR

Conspicuity and Evolution of Lesions in Creutzfeldt-Jakob Disease at Diffusion-Weighted Imaging

Takaki Murata, Yusei Shiga, Shuichi Higano, Shoki Takahashi and Shunji Mugikura

Conspicuity and Evolution of Lesions in Creutzfeldt-Jakob Disease at Diffusion-Weighted Imaging

Takaki Murata, Yusei Shiga, Shuichi Higano, Shoki Takahashi, and Shunji Mugikura

BACKGROUND AND PURPOSE: Diffusion-weighted imaging can disclose distinct hyperintense lesions in Creutzfeldt-Jakob disease (CJD). However, these findings and chronologic changes of CJD at diffusion-weighted imaging have not been fully investigated. Our purpose was to assess the diagnostic value of diffusion-weighted imaging in depicting CJD-related lesions and in tracking the evolution of these lesions. We also compared the sensitivity of diffusion-weighted imaging in depicting CJD-related lesions to that of fluid-attenuated inversion recovery (FLAIR) imaging.

METHODS: We reviewed findings in 13 patients with a diagnosis of CJD who underwent MR imaging, including diffusion-weighted imaging. Nine patients were initially examined within 4 months of onset of symptoms (early stage), and eight were examined 4 months or later (late stage). We evaluated four items: 1) distribution of lesions at diffusion-weighted imaging, 2) conspicuity of lesions at diffusion-weighted imaging and FLAIR imaging, 3) chronologic changes in lesions at diffusion-weighted imaging, and 4) chronologic changes in lesions revealed by apparent diffusion coefficient (ADC) maps.

RESULTS: Patients had striatal lesions or cerebral cortical lesions or both. The thalamus was involved in only one patient, and the globus pallidus was spared in all patients. The sensitivity of diffusion-weighted imaging in depicting lesions was superior or at least equal to that of FLAIR imaging. Hyperintense lesions at diffusion-weighted imaging changed in extent and intensity over time. Unlike infarction, lesional ADC decreased for 2 weeks or longer.

CONCLUSION: The progressively hyperintense changes in the striata and cerebral cortices at diffusion-weighted imaging are considered characteristic of CJD. Diffusion-weighted imaging may be useful for the early diagnosis of CJD.

Creutzfeldt-Jakob disease (CJD) is one of the subacute spongiform encephalopathies caused by a transmissible protein called a prion. The disease usually affects older adults and is inevitably fatal within 1 year of onset. CJD is clinically characterized by a rapidly progressive dementia, myoclonus, and periodic synchronous discharge (PSD) on electroencephalograms (EEGs). However, this triad is not always found in patients with CJD, especially in the early course of the disease; therefore, the diagnosis of CJD is difficult in the early stage. Several reports (1, 2) suggest

that bilateral, symmetric, diffuse hyperintensity in the basal ganglia on T2-weighted images may be a specific sign of CJD. The recent introduction of new pulse sequences such as those used in fluid-attenuated inversion recovery (FLAIR) imaging and diffusion-weighted imaging has enhanced the diagnostic usefulness of MR imaging. Compared with T2-weighted images, FLAIR images more clearly show lesions in the cerebral cortices and basal ganglia (3). Furthermore, diffusion-weighted imaging has been reported to depict characteristically distinct hyperintense lesions in CJD (4–8).

To our knowledge, chronologic changes in CJD at diffusion-weighted imaging have not been reported nor has the sensitivity of diffusion-weighted imaging in depicting lesional conspicuity in CJD been compared with that of FLAIR imaging. Our purpose was to clarify the evolution of CJD-related lesions as depicted with diffusion-weighted imaging and to evaluate the value of diffusion-weighted imaging in the diagnosis of CJD. We also compared the sensitivity of

TABLE 1: Patient data, clinical findings, and MR imaging results

Case No./Patient Sex/Age (y)	Dementia	Myoclonus	PSD	Prion Protein Gene	CDJ Type	Diagnostic Level	Diffusion-weighted Imaging	FLAIR Imaging	ADC Analysis
1/F/55	Yes	Yes	Yes	M232R	F	Definite	E(1), L(2)	E(1), L(2)	E(1), L(2)
2/M/78	Yes	No	No	V180I	F	Definite	L(2)	L(2)	L(2)
3/M/70	No	Yes	Yes	NA	S?	Probable	E(4), L(1)	E(1)	NA
4/M/66	Yes	Yes	Yes	Wild type	S	Probable	E(1), L(3)	E(1), L(3)	E(1), L(3)
5/M/60	Yes	No	Yes	Wild type	S	Probable	E(1), L(1)	E(1), L(1)	E(1), L(1)
6/M/58	Yes	Yes	Yes	E200K	F	Definite	L(3)	NA	NA
7/F/75*	Yes	No	No	Wild type†	S	Definite	L(1)	L(1)	L(1)
8/M/68	Yes	Yes	Yes	Wild type	S	Probable	E(2)	E(1)	NA
9/F/74	Yes	Yes	Yes	Wild type	S	Probable	L(1)	L(1)	L(1)
10/F/76	Yes	Yes	Yes	NA	S?	Probable	E(1)	E(1)	E(1)
11/M/78	Yes	Yes	Yes	NA	S?	Probable	E(1)	E(1)	E(1)
12/F/76	Yes	Yes	Yes	NA	S?	Probable	E(2)	E(2)	E(1)
13/F/82	Yes	No	No	V180I	F	Definite	E(1)	E(1)	E(1)

Note.—E200K indicates the change of codon 200 from glutamate to lysine; M232R, change of codon 232 from methionine to arginine; V180I, change of codon 180 from valine to isoleucine; NA, not available; F, familial; S, sporadic; S?, possibly sporadic; E, the early-stage study; L, late-stage study. The number in the parenthesis indicates the number of MR studies performed. Total numbers of examinations were as follows: diffusion-weighted imaging, 14 early stage and 14 late stage; FLAIR imaging, 10 early stage and 10 late stage; ADC imaging, seven early stage and 10 late stage.

* The diagnosis of CJD was confirmed at histopathologic analysis.

† Wild-type prion protein gene with valine homozygosity at codon 129.

TABLE 2: Summary of MR studies

Examination	Early Stage	Late Stage	Total
Diffusion-weighted imaging	9 (14)	8 (14)	13 (28)
Diffusion-weighted imaging with FLAIR imaging	9 (10)	6 (10)	12 (20)
ADC imaging	7 (7)	6 (10)	10 (17)

Note.—Data are the number of patients. Data in parentheses are the number of studies.

TABLE 3: Lesional distribution at Diffusion-weighted imaging

Site of Lesion	Early Stage (n = 9)	Late Stage (n = 8)
Striatum	8 (89)	8 (100)
Cortex	8 (89)	6 (75)
Thalamus	0 (0)	1 (12)
Globus pallidus	0 (0)	0 (0)

Note.—Data are the number of patients. Data in parentheses are percentages.

diffusion-weighted imaging in depicting CJD-related lesions with that of FLAIR imaging.

Methods

Subjects

We retrospectively reviewed findings in 13 patients who had a diagnosis of CJD (seven men, six women; age range, 55–82 years; mean age, 70 years) who were examined at MR imaging, including diffusion-weighted imaging. In one patient, the diagnosis was confirmed at histopathologic analysis. In four of the 13 patients, the familial type of CJD was confirmed by means of prion protein genetic analysis. Probable or definite CJD was eventually diagnosed in all patients by using clinical criteria (9). The approximate time of onset of symptoms in each patient was determined by chart review. Patient data, including clinical findings, are summarized in Table 1.

Data Acquisition

Imaging was performed using a 1.5- or 1.0-T MR units (Signa Horizon LX; GE Medical Systems, Milwaukee, WI or MAGNETOM Vision; Siemens, Erlangen, Germany) equipped with a conventional head coil. Subjects' heads were fixed symmetrically in the head coil with a band and cushions to reduce motion artifacts. Diffusion-weighted imaging was performed with single-shot spin-echo echo-planar imaging. Imaging parameters were as follows: 4700–5000/93–123/1 or 2 (TR/TE$_{eff}$/NEX), 10–15 axial sections of 5- or 6-mm section thickness with a 1.5–3.0-mm intersection gap, 128 × 128 matrix, 220- or 230-mm field of view, and a diffusion encoding strength (b

factor) of 1000 s/mm^2. Findings were evaluated at isotropic diffusion-weighted imaging. The apparent diffusion coefficient (ADC) maps were calculated on a workstation. FLAIR imaging parameters were 6000–9002/100–120/1700–2200 (TR/TE/TI), 5- to 7-mm section thickness, 1.5- to 3.0-mm intersection gap, 192 × 192 or 256 × 192 matrix, and 210–240-mm field of view.

Evaluation of Lesions

We defined the stage of the disease as follows: early stage, which was within 4 months of the onset of symptoms, and late stage, which was 4 months or later. All 13 patients were examined with diffusion-weighted imaging at least once, for a total of 28 studies. In the early stage, diffusion-weighted imaging was performed in nine patients (14 studies), and eight patients were examined with diffusion-weighted imaging in the late stage (14 studies). Four patients were examined in both the early stage and the late stage. FLAIR images obtained at the same examination or within 3 days of diffusion-weighted imaging were eligible for the comparative study (total of 20 studies in 12 patients). Nine patients were examined with FLAIR imaging in the early stage (10 studies), whereas six patients were examined with FLAIR imaging in the late stage (10 studies). The ADC maps were available in 10 patients (17 studies): seven patients (seven studies) and six patients (10 studies) were examined in the early stage and late stage, respectively. Four of the 10 patients were examined more than twice. The summary of the MR studies is listed in Table 2.

We evaluated four items. First, to assess the lesional distribution on diffusion-weighted images, we counted the number of hemispheres with the following: striatal (caudate or putami-

FIG 1. Case 1. Sample case of predominant striatal lesions in the early stage. Images were obtained at 3 (*A* and *B*) and 5 (*C* and *D*) months from the onset of symptoms.

A, FLAIR image shows changes, which are not as conspicuous as in *B*.

B, Striata appear hyperintense at diffusion-weighted imaging. Note that the anterior portion of the bilateral putamina (*arrows*) appears more hyperintense than does the posterior portion at diffusion-weighted imaging.

C and *D*, Severe atrophy is depicted in both cerebral cortices and the caudate nuclei heads at FLAIR imaging (*C*) and diffusion-weighted imaging (*D*). Note that the putamina are entirely involved in *C* as compared with their appearance in *B*. Hyperintensity in the heads of the caudate nuclei appears less prominent; this appearance is associated with their volume loss and the dilatation of the frontal horns.
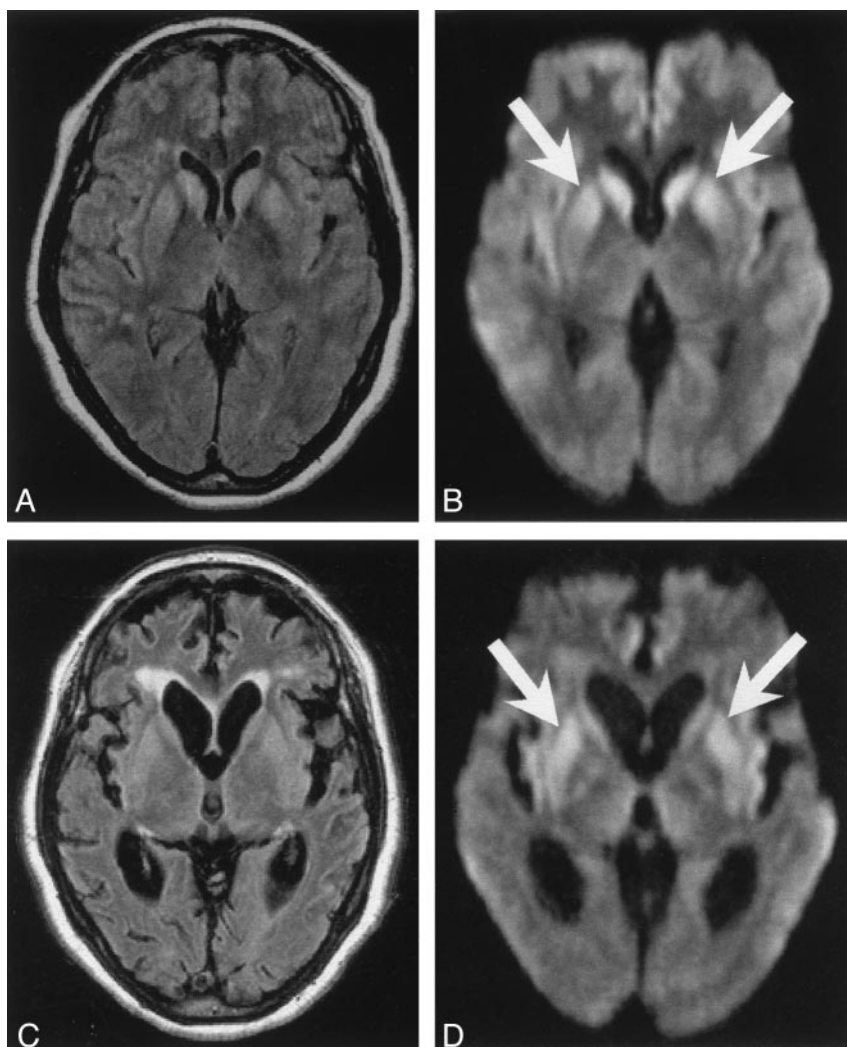
nal or both) lesions, cortical lesions, thalamic lesions, and lesions of the globus pallidus. When a patient was examined more than twice in the same stage, we evaluated the examination that revealed the most extensive lesions. Second, we compared diffusion-weighted imaging and FLAIR images for lesional conspicuity. In cases with cortical involvement in bilateral cerebral hemispheres, we evaluated each hemisphere individually (total of 28 hemispheres with cortical involvement in 10 patients). As for the striatum, we separately evaluated lesions in the caudate heads and the putamina, as distinguished on the right side compared with the left side in each hemisphere (total of 53 striatal lesions in 11 patients). We subjectively assessed lesional conspicuity and classified it as follows: 1) diffusion-weighted imaging was inferior to FLAIR; 2) diffusion-weighted imaging was equal to FLAIR; and 3) diffusion-weighted imaging was superior to FLAIR. Third, we evaluated chronologic lesional spread in eight patients who were examined with diffusion-weighted imaging more than twice (regardless of stage). We also evaluated the chronologic changes in the striatal lesions at diffusion-weighted imaging. We investigated the following three items: the pattern of progression of the striatal lesion, the direction of the spread of abnormal signal intensity in the putamen at diffusion-weighted imaging, and the relationship between caudate head lesions and ipsilateral putaminal lesions. Fourth, the chronologic changes on ADC maps were visually evaluated in the four patients in whom comparable ADC maps were available.

TABLE 4: Comparison of lesional conspicuity at diffusion-weighted imaging and FLAIR imaging

Site of Lesion	Category*			
	A	B	C	Total
Striatum				
Early	0	12	10	22 (7)
Late	2	12	17	31 (6)
Total	2	24	27	53 (11)
Cortex				
Early	0	3	11	14 (7)
Late	0	5	9	14 (4)
Total	0	8	20	28 (10)

Note.—Data are the number of lesions. Data in parentheses are the number of patients.

* We subjectively assessed lesional conspicuity and categorized it as follows: A, diffusion-weighted imaging was inferior to FLAIR; B, diffusion-weighted imaging was equal to FLAIR; and C, diffusion-weighted imaging was superior to FLAIR.

Two experienced neuroradiologists (S.T., S.H.) evaluated the MR studies, including those obtained at diffusion-weighted imaging and FLAIR imaging and the ADC maps. All images for each patient were reviewed side by side and findings were determined by consensus.
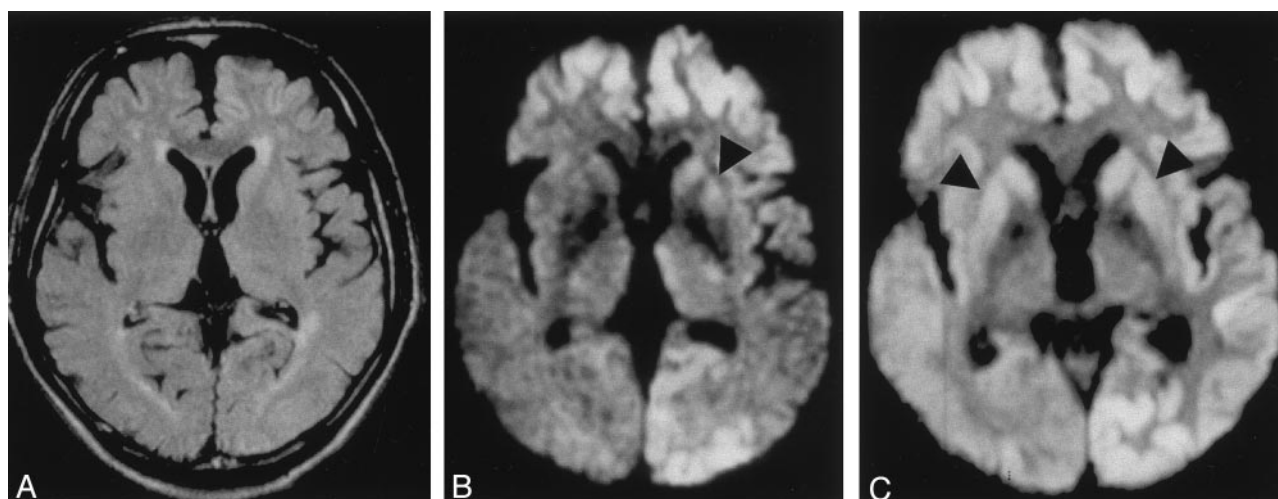
FIG 2. Case 3. Sample case in which cerebral cortices were involved mainly in the early stage.

A and *B*, At 1 month from the onset of symptoms, FLAIR imaging (*A*) reveals only subtle changes, whereas diffusion-weighted imaging (*B*) reveals hyperintense lesions in the cerebral cortices with a faint left striatal lesion. Note that the left striatum is asymmetrically involved (the right striatum is spared), and the anterior portion of the left putamen appears hyperintense compared with the posterior portion (*arrowhead* in *B*).

C, At 3 months from onset of symptoms, diffusion-weighted imaging reveals not only cortical lesions but also diffuse bilateral striatal lesions (*arrowheads*). Note that the left putaminal lesion spread posteriorly and entirely, as compared with its appearance in *B*.
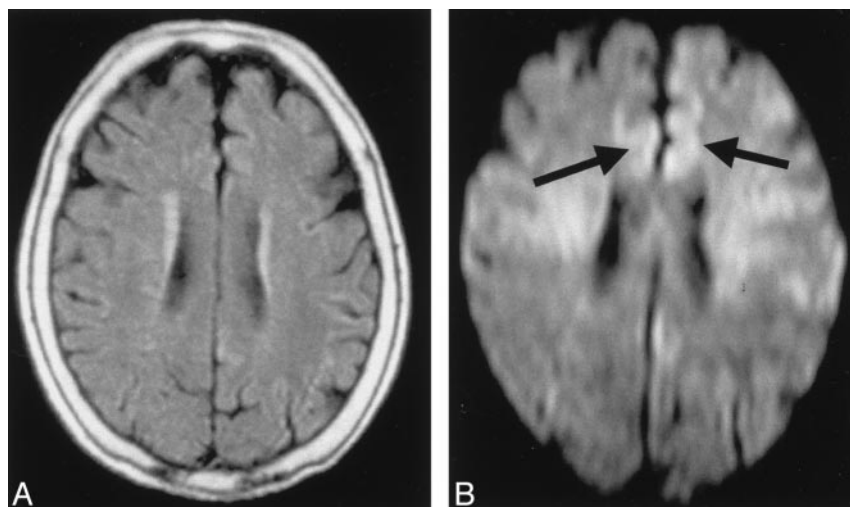

FIG 3. Case 13. Sample case in which a cortical lesion was apparent at diffusion-weighted imaging but not at FLAIR imaging. Images were obtained 2 months after onset of symptoms.

A, FLAIR image barely depicts the lesions shown in *B*.

B, Diffusion-weighted imaging reveals hyperintense cortical lesions in the medial aspects of bilateral frontal lobes.

Results

Lesional Distribution at Diffusion-Weighted Imaging

The percentage and number of patients with lesions in the striatum, cortex, thalamus, and globus pallidus in the early and late stages are summarized in Table 3. Most patients had both striatal and cerebral cortical lesions (Fig 1). The thalamus was involved in only one patient in the late stage. The globus pallidus was spared in all patients.

Comparison of Lesional Conspicuity at Diffusion-Weighted Imaging and FLAIR Imaging

The sensitivity of diffusion-weighted imaging to lesional conspicuity in both the early stage and the late stage was equal or superior to that of FLAIR imaging

(Table 4). However, two striatal lesions in one patient in the late stage were category A (ie, diffusion-weighted imaging was inferior to FLAIR). In this case, severe motion artifacts were noted at diffusion-weighted imaging, whereas artifacts were not as obvious at FLAIR imaging; these artifacts affected lesional conspicuity at diffusion-weighted imaging. Diffusion-weighted imaging revealed obvious high-signal-intensity abnormalities in the cerebral cortices or striatum or both. FLAIR imaging showed only subtle or barely detectable changes in two patients (Figs 2A and B and 3) or was of little diagnostic value because of severe motion artifacts in two other patients (Fig 4). The overall results, obtained by combining the results in the early stage with those in the late stage, also indicated that diffusion-weighted imaging was superior to FLAIR imaging, especially in the depiction of cortical lesions (Table 4).

FIG 4. Case 10. Sample case in which FLAIR imaging is of little diagnostic value because of severe motion artifacts. Images were obtained 2.5 months after the onset of symptoms.

A, Motion artifacts are so severe on the FLAIR image that it cannot provide diagnostic clues.

B, Diffusion-weighted imaging, however, clearly reveals hyperintense lesions (*arrows*) in right temporo-occipital cortices and cingulate gyrus.
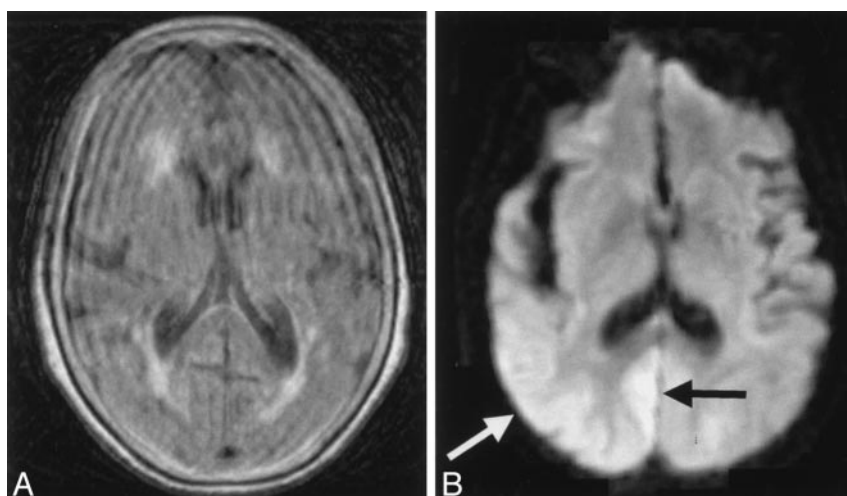

TABLE 5: Chronologic changes in striatal lesions

A: Progression pattern of striatal lesions*

Lesion	Initial Diffusion-weighted Imaging Study	Latest Diffusion-weighted Imaging Study
Asymmetric	4 (50)	1 (12)
Symmetric	4 (50)	7 (88)

B: Relationship between lesions†

Caudate Head Lesion	Initial Diffusion-weighted Imaging Study	Latest Diffusion-weighted Imaging Study
Without ipsilateral putaminal lesion	4	0
With ipsilateral putaminal lesion	11	15

Note.—The evaluation of chronologic changes involved data from eight patients with striatal lesions who were examined with diffusion-weighted imaging more than twice.

* Data are the number of patients (n = 8). Data in parentheses are percentages.

† Data are the number of caudate head lesions with or without ipsilateral putaminal lesion.

Chronologic Change at Diffusion-Weighted Imaging

All eight patients who were examined with diffusion-weighted imaging more than twice had a progressive or at least constant lesional distribution. Signal intensity increased in some of the lesions and decreased in others, but these still had abnormal hyperintensity. Lesions with decreased signal intensity were noted in four of the eight patients in the late stage. Two of the four patients had severe brain atrophy.

In four of the eight patients, asymmetric striatal lesions were depicted in the initial images. The latest MR studies in seven of the eight patients showed bilateral symmetric striatal involvement. The results of the initial and latest MR studies are summarized in Table 5A.

Diffusion-weighted imaging also revealed chronologic changes in the putaminal lesions. In five of eight patients who underwent repeat diffusion-weighted imaging, hyperintense lesions were restricted to the anteroinferior portion of the putamen in initial images. Subsequently, lesions spread in the posterior direction to the entire putamen (Fig 5). In the other three patients, the distribution of striatal lesions did not notably change.

We also noted that putaminal lesions always accompanied ipsilateral caudate head lesions. Even when the putaminal lesion was only subtle or not detectable, the entire ipsilateral caudate head was often hyperintense at diffusion-weighted imaging (in seven of 12 patients who had striatal lesions). We also counted the caudate head lesions with and those without putaminal lesions on the initial and latest diffusion-weighted imaging studies (Table 5B). In the latest diffusion-weighted imaging study, the ratio of caudate head lesions without putaminal lesions decreased, as compared with the ratio in the initial study.

Chronologic Changes in ADC Maps

The ADC maps were available in 10 patients, and four of the 10 were examined more than twice. The ADC in distinct hyperintense lesions at diffusion-weighted imaging decreased in all 10 patients (Figs 6 and 7), and this reduced diffusivity lasted 2 weeks or longer in all four patients with repeated ADC studies. In two patients, lesional ADC had decreased for 2 months (during the follow-up period).

Discussion

The classic triad of symptoms of CJD includes rapidly progressive dementia, PSD on EEGs, and myoclonic jerks. Not all parts of this triad may be present, especially in the early course of CJD; therefore, the early diagnosis of CJD is difficult. Biochemical examinations, such as the assessment for elevated levels of 14–3-3 protein (10) or neuron-specific enolase (11) in CSF, are now known to be useful in the diagnosis of CJD. On the other hand, neuroradiologic examinations have been considered to be less helpful in the diagnosis of CJD. Indeed, findings on CT scans
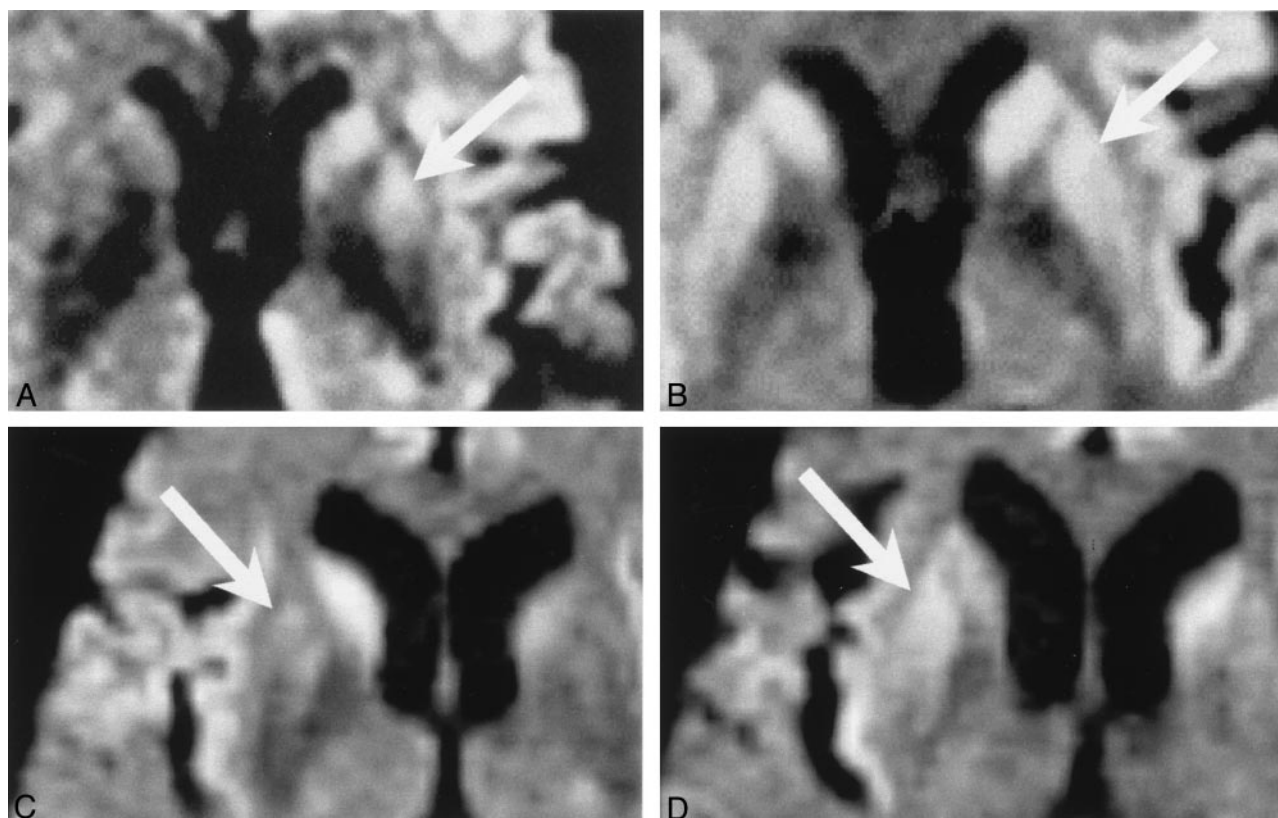
FIG 5. Cases 3 (*A* and *B*) and 5 (*C* and *D*). Sample cases with chronologic changes in striatal lesions (*arrow*).

A, At 1 month after the onset of symptoms, diffusion-weighted imaging reveals left striatal lesions. Note that the anterior portion of the left putamina appears more hyperintense than the posterior portion.

B, At 3 months after the onset of symptoms, diffusion-weighted imaging reveals that the left putaminal lesions spread posteriorly and entirely, as compared with the findings in *A*.

C, At 3 months after the onset of symptoms, diffusion-weighted imaging shows the right striatal lesion. Note that the high-signal-intensity change in the putamen is restricted to its anterior portion.

D, At 5 months after the onset of symptoms, diffusion-weighted imaging shows that the putaminal lesion has spread in the posterior direction, as compared with the findings in *C*.

are usually falsely negative for CJD (12), although they may indicate nonspecific diffuse brain atrophy in the late course of the disease (13). T2-weighted MR images depict basal ganglionic lesions in some cases of CJD (1, 2, 14), although these findings remain only subtle (15) and may be missed. The subsequent introduction of new pulse sequences such as those used in FLAIR imaging and diffusion-weighted imaging enhanced the diagnostic usefulness of MR imaging in CJD. Compared with T2-weighted imaging, FLAIR imaging more clearly shows lesions in the cerebral cortices and basal ganglia (3). Diffusion-weighted imaging reportedly reveals lesions in CJD to be characteristically and distinctly hyperintense (4–8).

Lesional Distribution at Diffusion-Weighted Imaging

Our patients eventually had striatal lesions or cerebral cortical lesions or both. On the other hand, the thalamus was involved in only one patient, and the globus pallidus was spared in all patients. These results clearly show that CJD has a high affinity for the striatum and the cerebral cortex but not for the thalamus or the globus pallidus. The cause of the char-

acteristic lesional distribution is not known as yet; however, we theorize that the histologic and anatomic differences among these structures might be one of the causes. The caudate nucleus and putamen are similar in structure; both are highly cellular and well-vascularized zones that are permeated by delicate bundles of either finely myelinated or nonmyelinated small-diameter fibers (16). In contrast, the globus pallidus is different from the corpus striatum in that it is encapsulated and traversed by numerous, coarse, heavily myelinated fibers (16). Differences in afferent connections are also known. The corpus striatum receives afferent fibers derived mainly from the cerebral cortex, thalamus, and substantia nigra, whereas afferent connections to the globus pallidus are derived principally from the corpus striatum (16).

Comparison of Diffusion-Weighted Imaging and FLAIR Imaging

To our knowledge, no comparative study of diffusion-weighted imaging and FLAIR imaging in CJD has been undertaken. Our results showed that diffusion-weighted imaging was superior or at least equal to FLAIR imaging in depicting lesions, especially those in
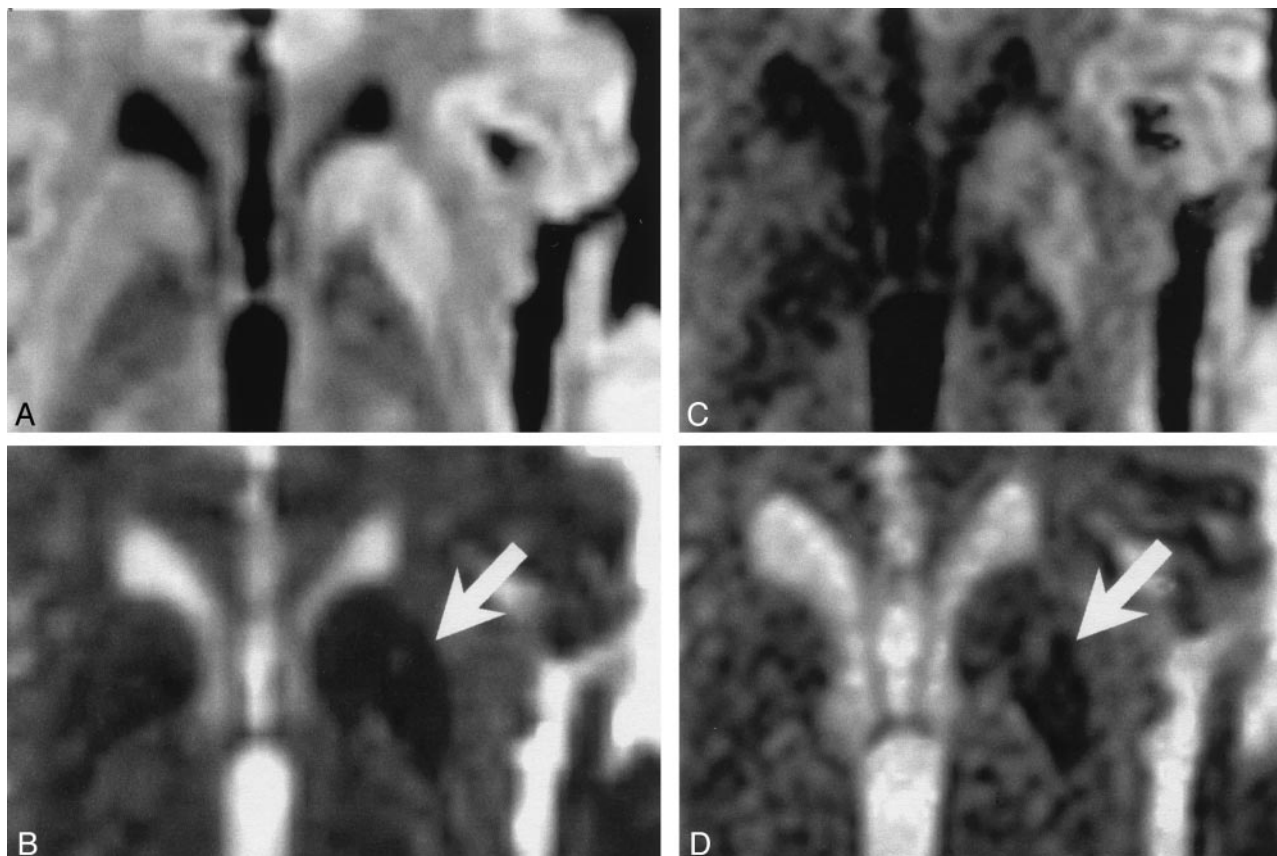
Fig 6.   Case 2. Sample case with chronologic changes in ADC in a striatal lesion.
 A and *B*, Diffusion-weighted imaging and corresponding ADC map, respectively. These images were obtained 7 months from the onset of symptoms. High signal intensity is present in the left striatum (*A*), and its lesional diffusivity is low (*arrow* in *B*).
 C and *D*, Diffusion-weighted imaging and corresponding ADC map, respectively. These images were obtained 8 months from the onset of symptoms. The lesion still has high signal intensity (*C*), and its ADC is still low (*arrow* in *D*).

the cortex (Table 4). Without diffusion-weighted imaging, some of these lesions might have been missed (Figs 2–4). One of the reasons for the superiority of diffusion-weighted imaging compared with FLAIR imaging may be its high contrast-to-noise ratio. In several cases, we calculated the contrast-to-noise ratios and confirmed that diffusion-weighted imaging was more than twice as good as FLAIR imaging (data not shown). High contrast-to-noise ratio at diffusion-weighted imaging would support the results of the comparative study. Another superiority of diffusion-weighted imaging is its short acquisition time. In this study, diffusion-weighted imaging was performed with single-shot echo-planar imaging that allowed the acquisition of images on the order of 100 milliseconds; therefore, diffusion-weighted imaging more effectively eliminated motion artifacts, as compared with FLAIR imaging. Diffusion-weighted imaging is considered valuable in examining patients, such as those with CJD, whose myoclonic jerks could possibly cause motion artifacts. However, unexpected motion causes artifacts, even with diffusion-weighted imaging.

Chronologic Change of Lesions Revealed by Diffusion-Weighted Imaging

All eight patients who were examined with diffusion-weighted imaging more than twice had a pro-

gressive or at least constant lesional distribution. According to these findings, we believe that diffusion-weighted imaging might have revealed the development of the disease.

With regard to the striatal lesions, initials studies in four of the eight patients showed asymmetric striatal lesions. The latest MR studies demonstrated that seven of the eight patients had bilateral, symmetric, striatal lesions. These findings indicate that striatal involvement might have begun focally or asymmetrically, and then subsequent lesional spread resulted in more extended symmetric involvement. Some (1) have reported that bilateral, symmetric, hyperintense abnormalities in the basal ganglia in T2-weighted images might be a specific sign of CJD. We suppose that diffusion-weighted imaging can reveal lesions in the striatum earlier and with more conspicuity than T2-weighted imaging; asymmetric but not symmetric striatal involvements were frequently detected with diffusion-weighted imaging.

Repeated diffusion-weighted imaging studies revealed chronologic changes in the putaminal lesion. That is, the hyperintense lesion tended to be restricted to the anteroinferior portion of the putamen on the initial study, and it subsequently spread in the posterior direction, and entire involvement of the putamen resulted (five of eight patients). We also
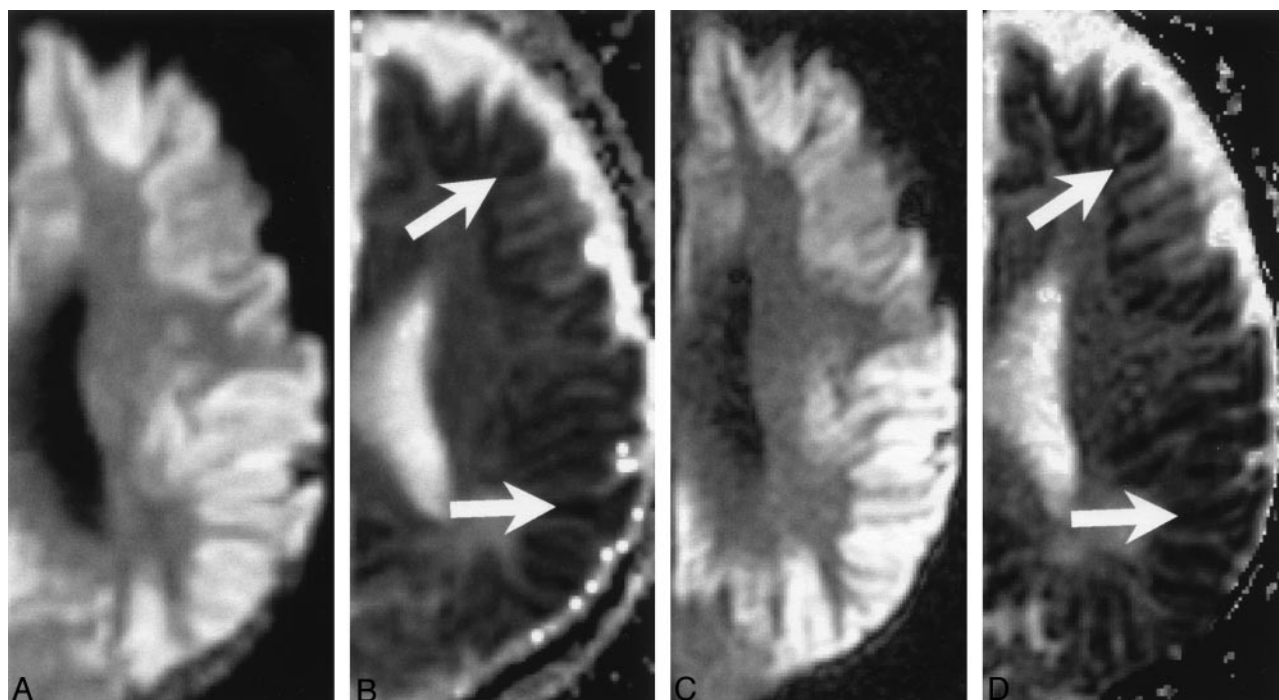
Fɪɢ 7. Case 2. Sample case with chronologic ADC changes in cerebral cortical lesions.

A and *B*, Diffusion-weighted imaging and corresponding ADC map, respectively. These images were obtained 7 months after the onset of symptoms. The cerebral cortices are hyperintense (*A*), and lesional ADCs are low (*arrows* in *B*).

C and *D*, Diffusion-weighted imaging and corresponding ADC map, respectively. These images were obtained 8 months after the onset of symptoms. The lesions are still hyperintense (*C*), and lesional ADCs are still low (*arrows* in *D*).
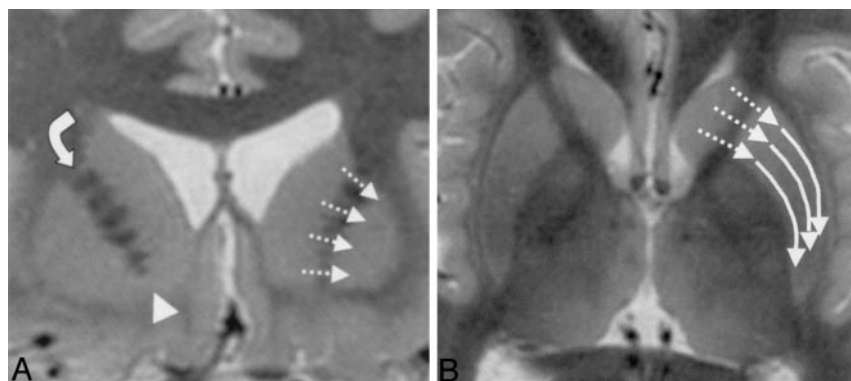

Fɪɢ 8. Short-TI inversion recovery images. *Dotted arrows* in the left striatum show the supposed pathway of lesional distribution along the putaminocaudate gray matter bridges and nucleus accumbens septi.

A, Coronal image shows the anatomic connections between the caudate head and the putamen. *Solid arrow* and *arrowhead* in the right cerebral hemisphere indicate the putaminocaudate gray matter bridges and the nucleus accumbens septi, respectively.

B, *Solid arrows* in the left putamen on this axial image show the direction of lesional extension observed in our study.

found that the putaminal lesion always accompanied by an ipsilateral caudate head lesion, whereas the converse was not necessarily true. Accordingly, we hypothesized that the caudate head lesion gradually extends to the ipsilateral putamen. This hypothesis may be supported by the fact that the anteroinferior portion of the putamen is continuous with the head of caudate nucleus (nucleus accumbens septi), and beside this anteroinferior connection, strands of gray matter (putaminocaudate gray matter bridges) connect the caudate head with the putamen (Fig 8A) (16). Meanwhile, findings from experimental studies of prion disease suggest an axonal transsynaptic spread of the disease (17–19). By taking these anatomic and experimental results into consideration, the chronologic changes in the striatum at diffusion-weighted imaging may suggest that the serial lesional spread from the caudate head to the putamen may

occur via direct connections between these two structures. Further posterior spread in the putamen may occur by means of an axonal transsynaptic pathway (Fig 8). However, we have no pathologic proof of these speculations, and further study is needed to make this conclusion.

Chronologic Changes on ADC Maps

Several reports of the value of ADC in CJD lesions exist. Some authors (5, 7) report a substantial decrease in ADC values, whereas others (8) reported no obvious abnormalities on ADC maps. Consistent with the former finding, ADCs in lesions that were hyperintense at diffusion-weighted imaging decreased in our study. This restricted diffusion lasted 2 weeks or longer, which was distinct from findings in infarction (20). The mechanisms of restricted diffusion remain

unknown at present. According to the findings from radiologic-pathologic correlation studies, marked astrogliosis is noted in hyperintense lesions at T2-weighted imaging (21) or diffusion-weighted imaging (8), whereas spongiform change is not prominent. However, other authors (5) argue that the presence of vacuoles in spongiform encephalopathy might have been the cause of the low ADC values.

Early Diagnosis of CJD

In this study, three patients (cases 2, 7, and 13) had neither PSD nor myoclonus during their entire clinical course. They had been given some tentative clinical diagnosis other than CJD before the initial MR study: in case 2, the tentative diagnosis was Parkinson disease, and the others had a diagnosis of nonspecific dementia. However, diffusion-weighted imaging revealed hyperintense cerebral cortical or striatal abnormalities or both; therefore, we suspected a diagnosis of CJD. Neurologists performed further investigations such as prion protein genetic analysis or CSF analysis, and the results led to the final diagnosis of CJD. Some (22) have reported that patients with a point mutation in the prion protein gene at the codon 180 locus (which changes valine to isoleucine) seldom have PSD, as shown on EEGs (case 2 and 13). Likewise, patients who have the wild-type prion protein gene with valine homozygosity at codon 129 locus rarely have PSD (case 7) (23, 24). We believe that diffusion-weighted imaging may contribute much in the early diagnosis of CJD, especially in patients without PSD.

Conclusion

The progressively hyperintense changes in the striata or cerebral cortices or both at diffusion-weighted imaging are considered characteristic of CJD. Diffusion-weighted imaging is useful in the early diagnosis of CJD.

Acknowledgments

References

1. Barboriak DP, Provenzale JM, Boyko OB. **MR diagnosis of Creutzfeldt-Jakob disease: significance of high signal intensity of the basal ganglia.** *AJR Am J Roentgenol* 1994;162:137–140
2. Finkenstaedt M, Szudra A, Zerr I, et al. **MR imaging of Creutzfeldt-Jakob disease.** *Radiology* 1996 Jun;199:793–798
3. Schwaninger M, Winter R, Hacke W, et al. **Magnetic resonance imaging in Creutzfeldt-Jakob disease: evidence of focal involvement of the cortex.** *J Neurol Neurosurg Psychiatry* 1997;63:408–409
4. Demaerel P, Baert AL, Vanopdenbosch L, Robberecht W, Dom R. **Diffusion-weighted magnetic resonance imaging in Creutzfeldt-Jakob disease.** *Lancet* 1997;349:847–848
5. Bahn MM, Kido DK, Lin W, Pearlman AL. **Brain magnetic resonance diffusion abnormalities in Creutzfeldt-Jakob disease.** *Arch Neurol* 1997;54:1411–1415
6. Yee AS, Simon JH, Anderson CA, Sze CI, Filley CM. **Diffusion–weighted MRI of right-hemisphere dysfunction in Creutzfeldt-Jakob disease.** *Neurology* 1999;52:1514–1515
7. Na DL, Suh CK, Choi SH, et al. **Diffusion-weighted magnetic resonance imaging in probable Creutzfeldt-Jakob disease: a clinical-anatomic correlation.** *Arch Neurol* 1999;56:951–957
8. Demaerel P, Heiner L, Robberecht W, Sciot R, Wilms G. **Diffusion-weighted MRI in sporadic Creutzfeldt-Jakob disease.** *Neurology* 1999;52:205–208
9. Kretzschmar HA, Ironside JW, DeArmond SJ, Tateishi J. **Diagnostic criteria for sporadic Creutzfeldt-Jakob disease.** *Arch Neurol* 1996;53:913–920
10. Hsich G, Kenney K, Gibbs CJ, Lee KH, Harrington MG. **The 14–3-3 brain protein in cerebrospinal fluid as a marker for transmissible spongiform encephalopathies.** *N Engl J Med* 1996; 335: 924–930
11. Wakayama Y, Shibuya S, Kawase J, Sagawa F, Hashizume Y. **High neuron-specific enolase level of cerebrospinal fluid in the early stage of Creutzfeldt-Jakob disease.** *Klin Wochenschr* 1987;65:798–801
12. Galvez S, Cartier L. **Computed tomography findings in 15 cases of Creutzfeldt-Jakob disease with histological verification.** *J Neurol Neurosurg Psychiatry* 1984;47:1244–1246
13. Kovanen J, Erkinjuntti T, Iivanainen M et al. **Cerebral MR and CT imaging in Creutzfeldt-Jakob disease.** *J Comput Assist Tomogr* 1985;9:125–128
14. Gertz HJ, Henkes H, Cervos-Navarro J. **Creutzfeldt-Jakob disease: correlation of MRI and neuropathologic findings.** *Neurology* 1988;38:1481–1482
15. Zeidler M, Will RG, Ironside JW, Sellar R, Wardlaw J. **Creutzfeldt-Jakob disease and bovine spongiform encephalopathy: magnetic resonance imaging is not a sensitive test for Creutzfeldt-Jakob disease.** *Br Med J* 1996;312:844
16. Gray H. *Gray's Anatomy.* 35th ed. London, England: Longman; 1973:976–979
17. Fraser H, Dickinson AG. **Targeting of scrapie lesions and spread of agent via the retino-tectal projection.** *Brain Res* 1985;346:32–41
18. Taraboulos A, Jendroska K, Serban D, Yang SL, DeArmond SJ, Prusiner SB. **Regional mapping of prion proteins in brain.** *Proc Natl Acad Sci U S A* 1992;89:7620–7624
19. Heye N, Cervos-Navarro J. **Focal involvement and lateralization in Creutzfeldt-Jakob disease: correlation of clinical, electroencephalographic and neuropathological findings.** *Eur Neurol* 1992;32:289–292
20. Burdette JH, Ricci PE, Petitti N, Elster AD. **Cerebral infarction: time course of signal intensity changes on diffusion-weighted MR images.** *AJR Am J Roentgenol* 1998;171:791–795
21. Urbach H, Klisch J, Wolf HK, Brechtelsbauer D, Gass S. Solymosi L. **MRI in sporadic Creutzfeldt-Jakob disease: correlation with clinical and neuropathological data.** *Neuroradiology* 1998;40:65–70
22. Ishida S, Sugino M, Koizumi N, et al. **Serial MRI in early Creutzfeldt-Jacob disease with a point mutation of prion protein at codon 180.** *Neuroradiology* 1995;37:531–534
23. Kitamoto T, Tateishi J. **Human prion diseases with variant prion protein.** *Philos Trans R Soc Lond B Biol Sci* 1994;29;343:391–398
24. Kovacs GG, Head MW, Bunn T, Laszlo L, Will RG, Ironside JW. **Clinicopathological phenotype of codon 129 valine homozygote sporadic Creutzfeldt-Jakob disease.** *Neuropathol Appl Neurobiol* 2000;26:463–472